Separation Science and Technology
Publication details, including instructions for authors and subscription information:
http://www.informaworld.com/smpp/title~content=t713708471

Study of *Saccharomyces cerevisiae* Yeast Cells by Field-Flow Fractionation and Image Analysis

M. N. Pons[a]; A. Litzén[b]; G. M. Kresbach[b]; M. Ehrat[b]; H. Vivier[a]
[a] LABORATOIRE DES SCIENCES DU GÉNIE CHIMIQUE, NANCY, CEDEX, FRANCE [b] BIOANALYTICAL RESEARCH CORPORATE RESEARCH UNITS CIBA-GEIGY LTD., BASEL, SWITZERLAND

To cite this Article Pons, M. N. , Litzén, A. , Kresbach, G. M. , Ehrat, M. and Vivier, H.(1997) 'Study of *Saccharomyces cerevisiae* Yeast Cells by Field-Flow Fractionation and Image Analysis', Separation Science and Technology, 32: 9, 1477 — 1492
To link to this Article: DOI: 10.1080/01496399708004061
URL: http://dx.doi.org/10.1080/01496399708004061

SEPARATION SCIENCE AND TECHNOLOGY, 32(9), pp. 1477–1492, 1997

Study of *Saccharomyces cerevisiae* Yeast Cells by Field-Flow Fractionation and Image Analysis

M. N. PONS*
LABORATOIRE DES SCIENCES DU GÉNIE CHIMIQUE
CNRS-ENSIC-INPL
1, RUE GRANDVILLE BP 451, F-54001 NANCY CEDEX, FRANCE

A. LITZÉN,† G. M. KRESBACH, and M. EHRAT
BIOANALYTICAL RESEARCH
CORPORATE RESEARCH UNITS
CIBA-GEIGY LTD.
CH-4002 BASEL, SWITZERLAND

H. VIVIER
LABORATOIRE DES SCIENCES DU GÉNIE CHIMIQUE
CNRS-ENSIC-INPL
1, RUE GRANDVILLE BP 451, F-54001 NANCY CEDEX, FRANCE

ABSTRACT

Asymmetrical flow field-flow fractionation has been applied to characterize *Saccharomyces cerevisiae* cells, the morphology of which has been assessed by image analysis during fermentation on glucose medium. Intact cells, budding or nonbudding, are eluted and separated according to the steric-hyperlayer modes, while macromolecules and other cell debris are eluted according to the normal mode.

INTRODUCTION

Field-flow fractionation (FFF) is a family of separation techniques suitable for the fractionation of molecules and particles in the size range from about 1000 in molecular weight to 50 μm in particle diameter (1). The flow

* To whom correspondence should be addressed.
† Present address: Astra Hässle AB, S-43183 Mölndal, Sweden.

FFF methods are based on the concept of a laminar flow profile in a channel through which an aqueous carrier is pumped. A field is applied perpendicular to the channel and interacts with the sample components, depending upon their characteristics (Fig 1a). In asymmetrical flow FFF, the retaining field is created by a crossflow, perpendicular to the axial flow, through the porous lower wall of a thin flat channel. The opposite upper wall is made of a glass plate (Fig. 1b and c). In the normal mode the selectivity is based on differences in the diffusion coefficient, and the samples are separated according to size and shape.

Depending upon the particle size, two different phenomena take place in the chamber: the Brownian normal mode applies to the smaller (submicronic) particles, and the lift-hyperlayer mode to the larger particles. The

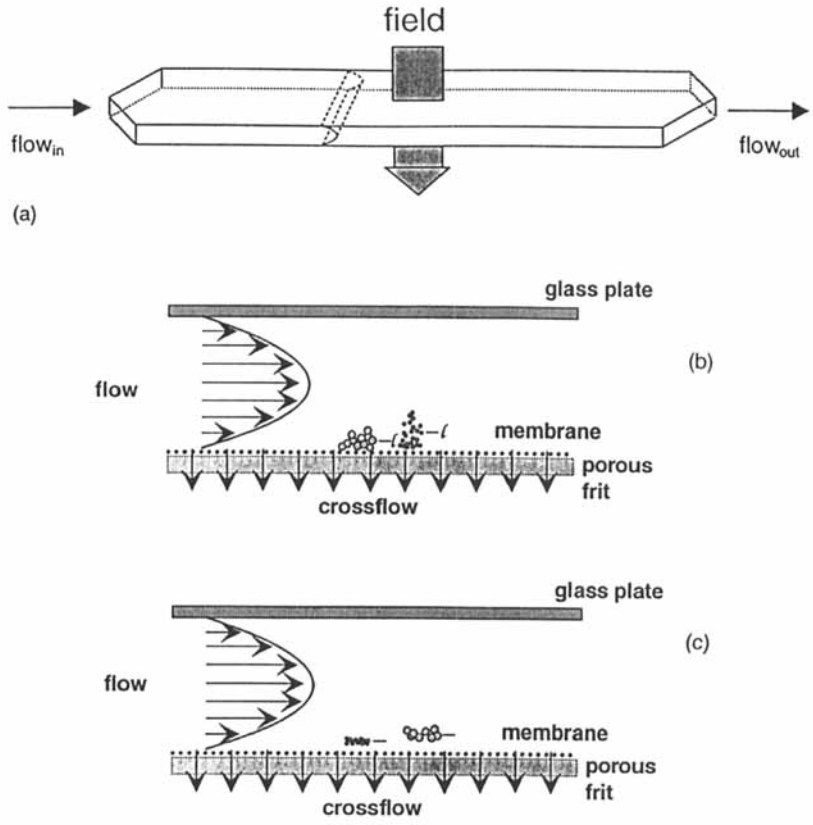

FIG. 1 (a) Principle of FFF. (b) Normal mode. (c) Lift-hyperlayer mode.

normal mode (Fig. 1b) is based on the balance reached between crossflow-induced convection, driving particles or molecules toward the accumulation wall, and molecular diffusion in the opposite direction. Under this mode the sample components elute in order of decreasing diffusion coefficient, i.e., the smallest components elute first. The lift-hyperlayer effect (Fig. 1c) takes place when the average distance from the accumulation wall, as predicted by the convection-diffusion balance, is exceeded by the particle radius. The hydrodynamic lift-forces play an important part in the mechanism causing the distribution of particles across the channel's thickness dimension (Fig. 1c). As a result, under this mode the largest particles exhibit a larger velocity and elute first. Samples containing a wide range of particle sizes may be subject to both mechanisms.

Flow FFF has been used to separate biomaterials of very different natures such as proteins (2, 3), viruses (4), antibodies (5), red blood cells (6), and plasmids or unicellular algae (7). In the latter case, fractograms of mixed populations were obtained, but the identity of the microorganisms in the different peaks could not be fully checked.

The purpose of this contribution is to examine whether asymmetrical flow FFF is suitable to characterize *Saccharomyces cerevisiae* cells (diameter $\approx$ 10 μm) during fermentations on glucose, using optical microscopy and image analysis to elucidate the obtained fractograms.

MATERIALS AND METHODS

Culture Conditions

A wild strain of *Saccharomyce cerevisiae* LBGH1022 was obtained from Botainisches Institut, Basel University, and stored in liquid nitrogen in cryovials. Cells were cultivated in 250 mL Erlenmeyer flasks equipped with a gauze stopper and placed on a shaker under a thermostated hood. Each flask contained 100 mL of basic culture medium and a proper amount of a 70% w/w glucose solution. Four cultures were run with different initial glucose concentrations: L10 (5 g/L), L11 (11 g/L), L7 (12.5 g/L), and L12 (21 g/L).

The basic culture medium contained, per liter: 4 g $(NH_4)_2SO_4$, 0.58 g KCl, 0.3 g $MgSO_4 \cdot 7H_2O$, 1.28 g $(NH_4)_2HPO_4$, 0.18 g $CaCl_2 \cdot 2H_2O$, 760 μL trace elements solution, and 1.5 mL vitamins solution. The trace elements solution contained, per liter: 2.34 g $CuSO_4 \cdot 5H_2O$, 14.6 g $FeCl_3$, 9 g $ZnSO_4 \cdot 7H_2O$, and 10.5 g $MnSO_4 \cdot H_2O$. The vitamins solution contained per liter: 15 g Ca-panthothenate, 30 g myo-inositol, 3 g thiaminhydrochloride, 0.82 g pyridoxolhydrochloride, and 0.016 g (+)-biotin.

Samples were taken regularly. Optical density was measured on a Lambda2 spectrophotometer (Perkin-Elmer, Uberlingen, Germany). Glu-

cose, acetaldehyde, and acetic acid were determined by enzymatic assays (refs 716 251, 668 613, and 148 261 respectively, from Boehringer Mannheim, Mannheim, Germany). Ethanol and other volatile components were determined using the Biomonitor (a Ciba proprietary system composed of a head-space purge-and-trap system, GC and hyphenated MS, with FT-IR and FID detectors). Sample pH was measured with a pH probe (Ingold micro Type U402-M3-57, Ingold, Urdorf, Switzerland) connected to a Metrom 632 pHmeter (Metrom, Herisau, Switzerland).

Cells debris were obtained by vigorous sonication of full cells (Branson Sonifier 250, Branson, Danbury, CT, USA). Viability was checked by methylene blue exclusion and cell counting.

Image Analysis

Cells from full broth and FFF eluate fractions (those were concentrated by centrifugation before examination) were observed by phase contrast light microscopy (Zeiss Labor Mikroskop, Zeiss, Oberkochen, Germany) (magnification $\times 100$). A monochrome CCTV Hitachi video camera was fitted to the microscope. Images (256 lines of 256 pixels) on 256 grey levels were grabbed via a PIP1024 Matrox board on a Datacube 486-2 $\times$ 33MHz computer. Visilog 4.1.3. (Noésis, Orsay, France) image analysis software was used under Windows on a PC-compatible. Additional software was written in C. Images were intermediately stored on tapes (VIP Archive,

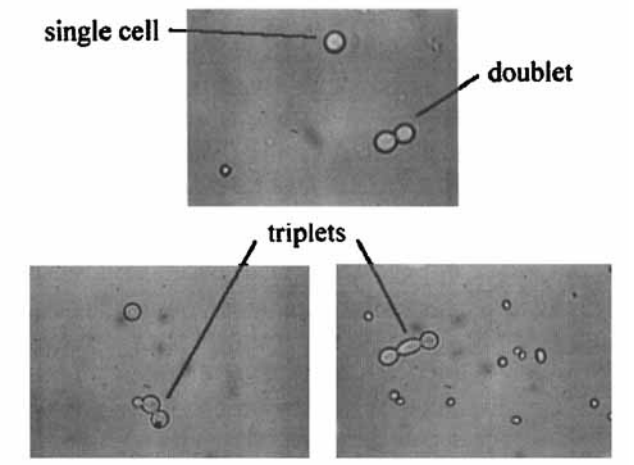

FIG. 2 Illustration of the different types of *Saccharomyces cerevisiae* cells.

Singapore) for later analysis. A graticule was used for pixel size calibration.

Image analysis of yeast cells has been previously described (8). Figure 2 presents typical images of single cells, doublets, and triplets. A doublet is constituted of a mother cell and an nondetached daughter cell. A triplet is constituted of a mother cell with two daughter cells. The purpose of the image analysis is to compute the number of cells (single, doublets, triplets), their size (equivalent diameter $D_{eq} = 2\sqrt{A/\pi}$, where A is the projected area) and their shape. Macroscopic shape descriptors were used: circularity ($= P^2/(4\pi A)$, where P is the projected perimeter), F_{max}/F_{min}, where F_{max} and F_{min} are respectively the maximal and minimal Feret diameter, and a/b, the ratio of the major axis to the minor axis of the ellipse equivalent to the cell projection. The percentages of single cells (%S) and of doublets (%D) are defined as:

$$\%S = \frac{\text{number of single cells}}{\text{total number of cells}}$$

$$\%D = \frac{\text{number of doublets}}{\text{total number of cells}}$$

200 to 300 cells per sample are examined.

FFF System

An asymmetrical flow FFF channel was constructed and housed (Fig. 3). It was similar to that described by Litzén et al. (5). The separation channel has a rectangular geometry with a length of 28.5 cm and a breadth of 1.5 cm. The reduction area at the inlet end was 1.12 cm^2, the thickness 0.019 cm, and the nominal volume 0.78 mL. The ultrafiltration membrane making up the accumulation wall was made of regenerated cellulose (type NADIR UF-C-10 from Hoechst AG, Wiesbaden, Germany).

The experimental set-up was similar to that described in Litzén et al. (5). Pump 1 was a Gynkotek M480 HPLC pump (Gynkotek GmbH, Germering b. München, Germany) and pump 2 was a Synkam model S1000 solvent delivey system (Stagroma, Wallisellen, Switzerland). Detection was conducted at 610 nm with a Linear UVIS 206 detector (Spectra Physics, San Jose, CA, USA). Injection was made from a Rheodyne 9125 injector (Rheodyne Inc., Cotati, CA, USA) equipped with a 50-μL loop. Two electrically motor-driven valves directed the flows in the system. V1 was a E-CST 4 UV multiposition valve and V2 a WE-C8W 2-position valve (both from Valco Europe, Schenkon, Switzerland). The needle valve N1 was of type Nupro SS-SS1-A with micrometer head Ny-5K-S (Nupro, Willoughby, OH, USA). The flow rate through the channel outlet was

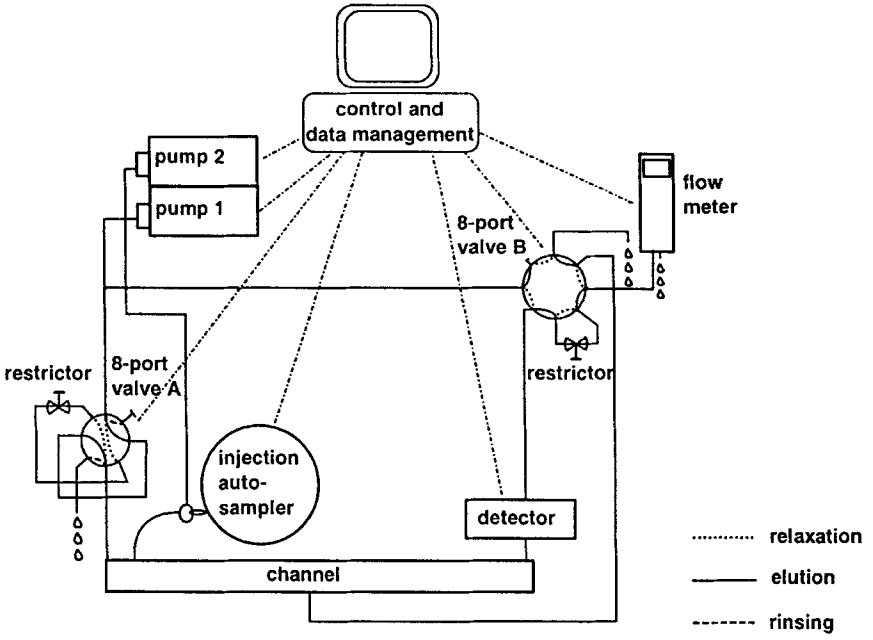

FIG. 3 Schematic drawing of asymmetrical flow FFF instrumentation.

measured by a Phasesep flowmeter with a 12-bit resolution analogue output (Phase Separations Ltd., Queensferry, UK); control and data acquisition was conducted by a GynkoSoft chromatography data system (Gynkotek GmbH). Both the UV signal (UV) and the flowmeter readings were monitored.

For the automated operation of the asymmetrical flow FFF system for yeast fractionation, the following flow rates (PBS pH 7.0 carrier) and times were used. The initial rinsing phase was maintained during 0.8 minute with pump 1 flushing the channel backward at a flow rate of 1 mL/min. The injection-relaxation-focusing phase lasted 1 minute with the relaxation flow rate, V_c', of 2 mL/min delivered by pump 1. The sample (volume 50 μL) was injected during the first 45 seconds at a flow rate of 0.2 mL/min (delivered by pump 2). The focusing point was adjusted to 2 cm from the channel inlet (0.5 cm downstream from the injection inlet). During the elution, pump 1 delivered a flow rate of 3 mL/min (V_{in}), which was divided to crossflow (V_c = 1.27 mL/min) and outlet flow rate (V_{out} = 1.73 mL/min).

For calibration, polystyrene latex beads (Seradyn, Indianapolis, IN, USA) of diameters 3, 7, and 15 μm were fractionated using a (0.1% SDS + 0.02% NaN_3) carrier.

Cells fractograms were characterized by their mean time (T_{mean}), mode time (T_{mode}), and variation coefficient (= standard deviation σ/T_{mean}) in the 0.6–3 minutes range after injection:

$$T_{mean} = \frac{\int_{0.6}^{3} UV(t)\cdot t\cdot dt}{\int_{0.6}^{3} UV(t)\cdot dt}$$

$$\sigma^2 = \frac{\int_{0.6}^{3} UV(t)\cdot[t - T_{mean}]^2\cdot dt}{\int_{0.6}^{3} UV(t)\cdot dt}$$

RESULTS

In order to test the separation performance of the FFF channel, polystyrene latex beads were fractionated using basically the same experimental conditions. Figure 4 demonstrates that the beads were easily separated and that the resolution increases with decreasing diameter. The order of elution was checked by separate experiments.

Figure 5(a) presents the general kinetics of fermentation L7, while the results of image analysis obtained on the full broth and the characteristics of FFF fractograms are given in Figs. 5(b) and 5(c), respectively. Up to $t = 20$ hours, the fractogram's statistical characteristics (mean time, mode time, and variation coefficient) are constant, with equal values for the

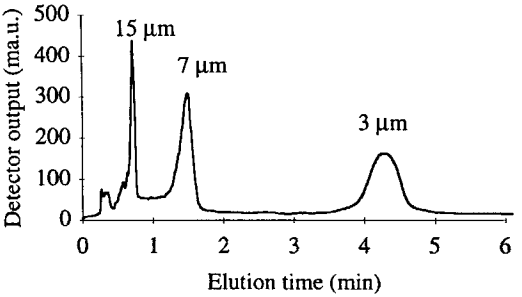

FIG. 4 Fractogram of polystyrene latex beads.

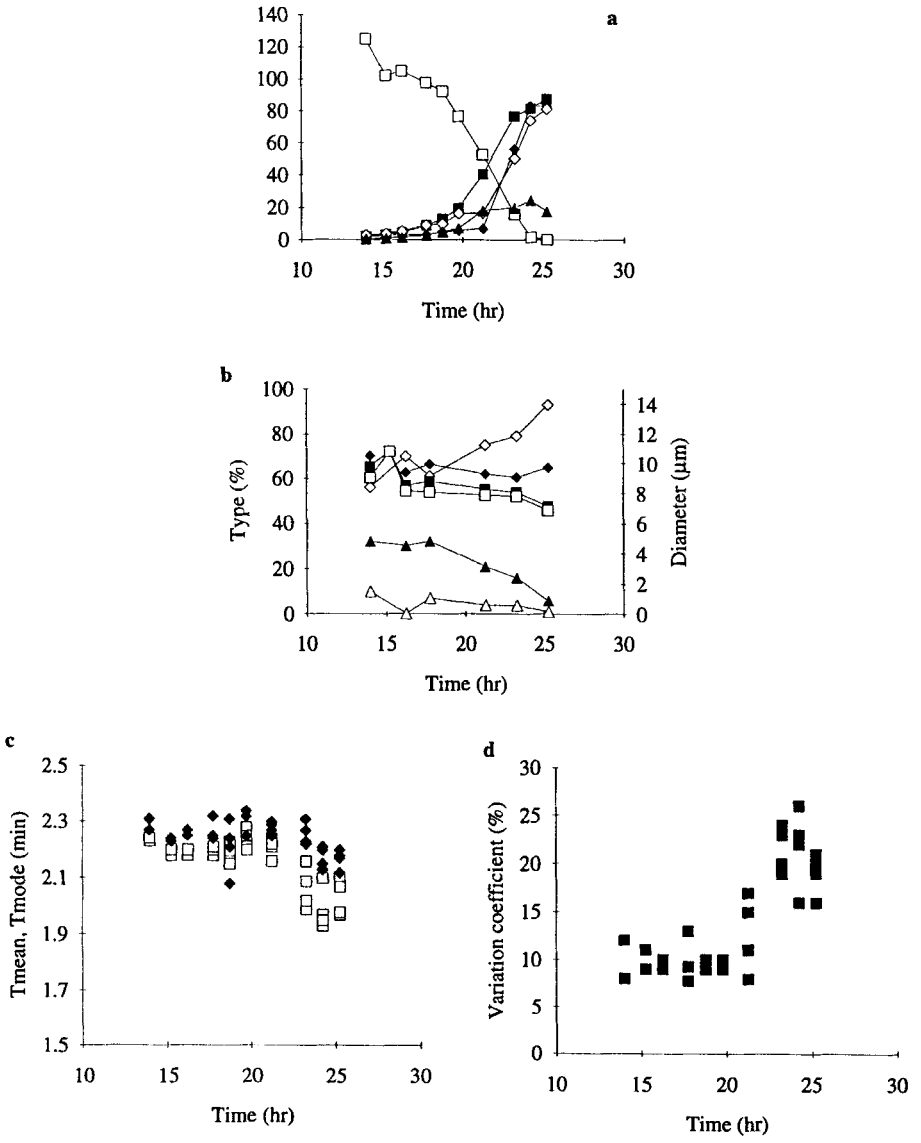

FIG. 5 Experiment L7. (a) General kinetics: (■) optical density (a.u.) × 10; (□) glucose (g/L) × 10; (◆) acetaldehyde (mg/L); (◇) acetate (mg/L); (▲) ethanol (g/L) × 10. (b) Image analysis results: (◇) % and (□) D_{eq} of single cells; (▲) % and (◆) D_{eq} of doublets; (Δ) % and (■) D_{eq} of triplets. FFF results: (c) (□) T_{mean}; (◆) T_{mode}. (d) (■) Variation coefficient.

mean and mode times. During that period the fractions of cells considered as single cells (nonbudding cells and mother cells exhibiting a small bud) and doublets (mother cells exhibiting a large bud) are also constant (65 and 30%, respectively). It was found that the average diameter for all type of cells was almost identical and that the doublets were only slightly bigger (Fig. 5b). As flow FFF separation is based on effective diameter, a good separation of single cells, doublets, and triplets will require a very fine setting of the operation conditions. If we model a doublet by two juxtaposed spheres of the same diameter D (i.e., mother cell of the same size as the daughter cell), the equivalent diameter given by image analysis (based on projected area) is

$$D_{eq} = 2\sqrt{\frac{2}{\pi}\frac{\pi D^2}{4}} = D\sqrt{2} = 1.41D$$

where $D = D_{daughter} = D_{mother}$. In terms of volume, the volume equivalent diameter of a doublet is

$$D_{eq.v} = D\sqrt[3]{2} = 1.26D$$

In the actual case, $D_{daughter} \leq D_{mother}$. Glucose concentration is not limiting, and almost no acetate or acetaldehyde are produced. After 20 hours the fractogram variation coefficient increases suddenly (Fig. 5d) and the mean time becomes smaller than the mode time (Fig. 5c): this indicates a modification of the shape of the fractograms. During that period the doublets fraction decreases, indicating a decrease of growth, and production of acetate and acetaldehyde is noticeable. After 25 hours, no glucose can be found in the broth.

Figure 6 gives more detailed informations on the fractograms obtained during fermentation L7. Until 20 hours they are characterized by a single, rather narrow peak (elution time range 1.75–2.6 minutes). Examination of different peak fractions by image analysis indicates that larger cells are eluted first: the equivalent diameter decreases as the elution time increases, confirming that the cells are eluted according to the steric-hyperlayer mode. However, both single cells and doublets are widely coeluted and there is, at least under the operation conditions used here, no full separation between budding and nonbudding cells. After 20 hours a second peak is noticeable on the fractograms at shorter elution times ($\approx$1.2 minutes). No yeast cells could be detected on fractions taken at that moment, but very small objects could be observed.

The three other fermentations confirm these trends: the fractograms exhibit a single peak (elution time range 1.75–2.6 minutes) up to the moment where a significant release of acetaldehyde and acetate is observed.

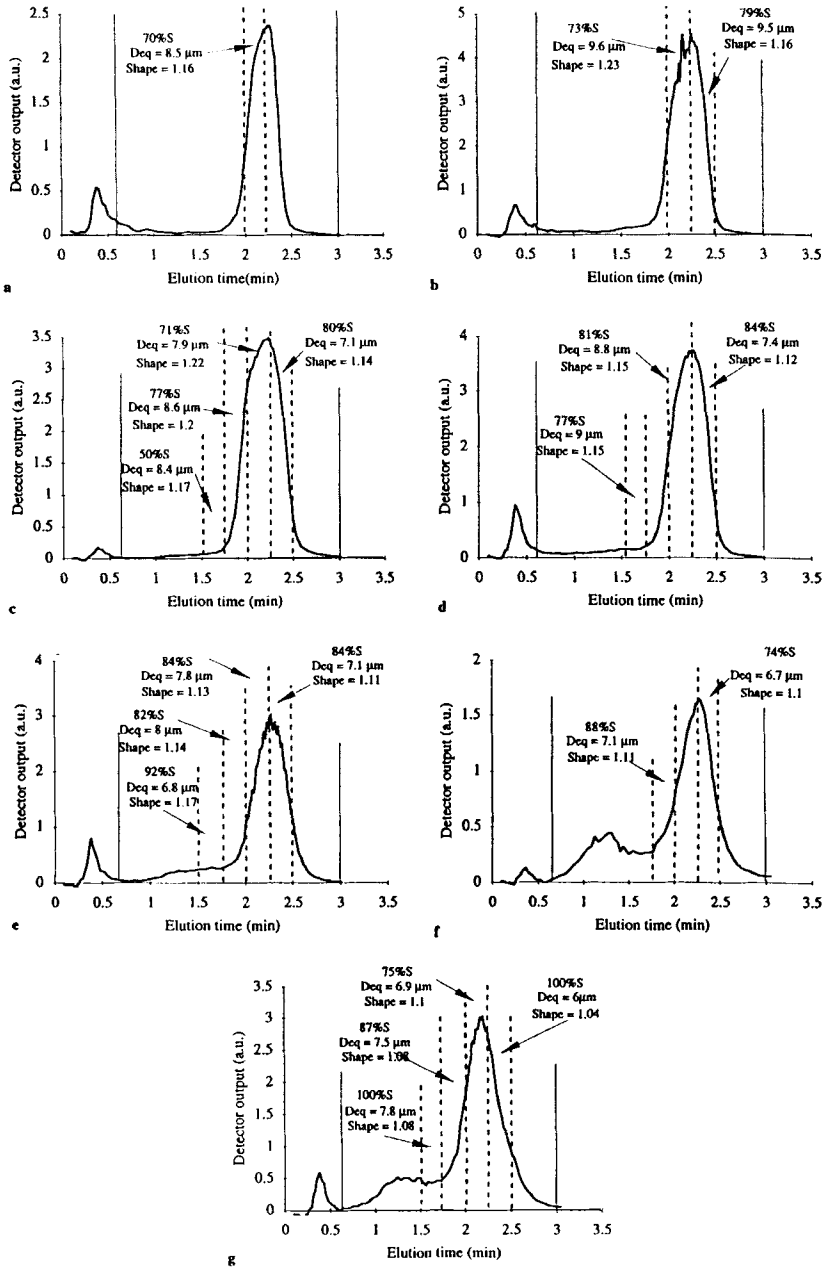

FIG. 6 Image analysis characterization of fractograms fraction during experiment L7: (a) 16.25 hours; (b) 17.75 hours; (c) 18.75 hours; (d) 19.75 hours; (e) 21.25 hours; (f) 23.25 hours; (g) 25.25 hours.

Then a second peak is observed at smaller elution times. Fermentation L10, run with a initial low concentration of glucose, was allowed to continue after glucose depletion: due to the low biomass concentration, oxygen was not limiting and growth on ethanol could be observed. Ethanol, acetaldehyde, and acetate were consumed (Fig. 7a). During this stage the fraction of doublets increased slightly and the fractograms variation coefficient decreased (Fig. 7b). In Experiment L11, just after the end of initial glucose consumption, some glucose was fed to the cells at 24.5 hours (Fig. 8a): a second growth phase could be noticed with a slight

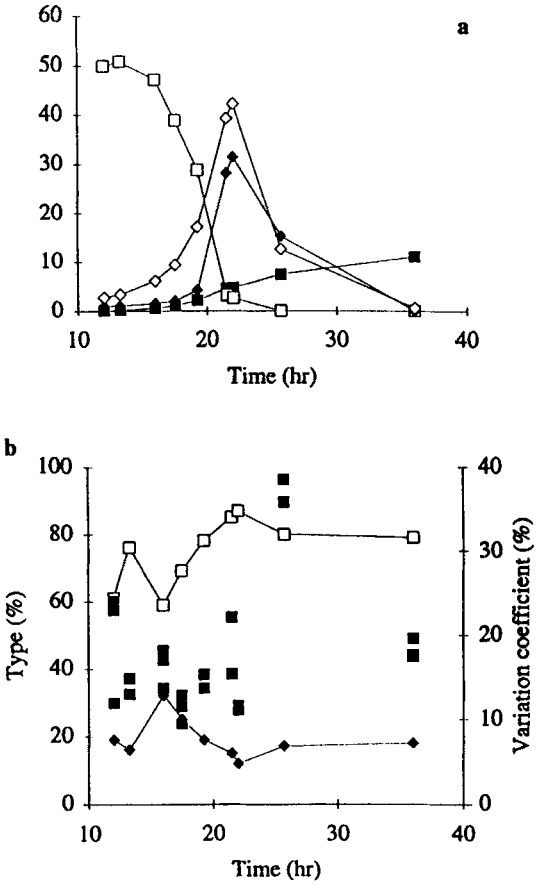

FIG. 7 Experiment L10. (a) General kinetics: (■) optical density (a.u.) × 10; (□) glucose (g/L) × 10; (◆) acetaldehyde (mg/L); (◇) acetate (mg/L). (b) Image analysis {(□) % single cells, (◆) % doublets} and FFF results {(■) variation coefficient}.

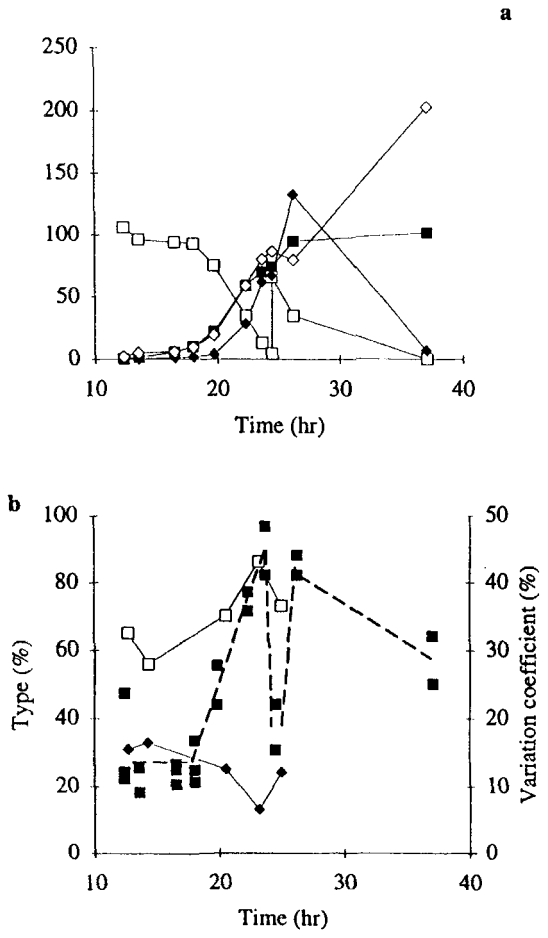

FIG. 8 Experiment L11. (a) General kinetics: (■) optical density (a.u.) × 10; (□) glucose (g/L) × 10; (◆) acetaldehyde (mg/L); (◇) acetate (mg/L). (b) Image analysis {(□) % single cells, (◆) % doublets} and FFF results {(■) variation coefficient}.

increase of the doublets fraction. For a short time period the fractogram variation coefficient decreased (Fig. 8b). Simultaneously the acetaldehyde and acetate production decreased.

Although the viability given by methylene blue exclusion ranged between 80 and 90%, it became evident that there was a relationship between the appearance of the second peak at short elution times and the cell's lysis. When the cells are dying, acetaldehyde and acetate are released

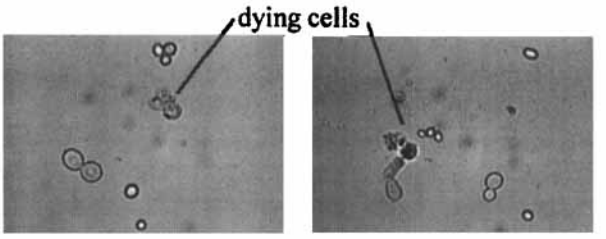

FIG. 9 Illustration of dying cells.

in larger amounts in the broth, either due to a increase of membrane permeability or to complete membrane breakage. When the cell membrane is disrupted, membrane fragments and various organelles and macromolecules are released in the broth. This can be seen on Fig. 9 which shows a wreath of intracellular materials exiting the membranes. To confirm this interpretation, a sample of fully growing cells was taken and the cells were submitted to sonication until only cells debris could be seen under the microscope. The corresponding FFF fractogram is given in Fig. 10, with a single peak around 1 minute. The various components, of small size, are eluted according to the normal mode.

The lift-hyperlayer mode and especially the hydrodynamic lift forces involved are not understood very well, so use of size standards as well

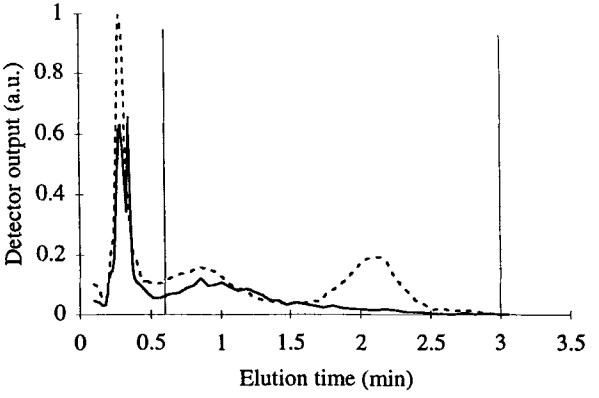

FIG. 10 Fractogram of sonicated full broth sample: (- - -) fractogram before sonication; (——) fractogram after sample dilution and sonication.

as correction factors are mandatory for a correct calibration based solely on FFF data. As neither standards related to yeast cells nor appropriate correction factors were available for this purpose, we attempted to compare latex standards with yeast cells experiments.

The yeast fractogram mean times (T_{mean}) were plotted versus the equivalent diameter derived from image analysis (Fig. 11). Values obtained from polystyrene-latex particles (fractionated using a different carrier) were added to this plot. The data obtained for the yeast cells were in coarse correspondence with those expected for particles of the same size. Several factors could account for the deviations rendered visible in Fig. 11. Particle–membrane interaction is not totally negligible in flow FFF, and the largely different surface characteristics of yeast cells and of polystyrene latex particles will have a strong impact on that interaction. In contrast to the spherical and monodisperse polystyrene latex particles, the cell populations exhibit a continuous distribution of shape and size factors: single cells and doublets show an average circularity of 1.15 and 1.3, an average F_{max}/F_{min} ratio of 1.5 and 1.8, and an average a/b ratio of 1.8 and 2.2, respectively.

Finally, Fig. 12 compares the variations of broth optical density and of the integrated FFF signal versus time for Experiment L7. Both curves exhibit a very similar pattern up to 20 hours. After that time the difference is due to the secondary peak in FFF fractograms. To a certain extent it is possible to use the integrated FFF signal to monitor the biomass

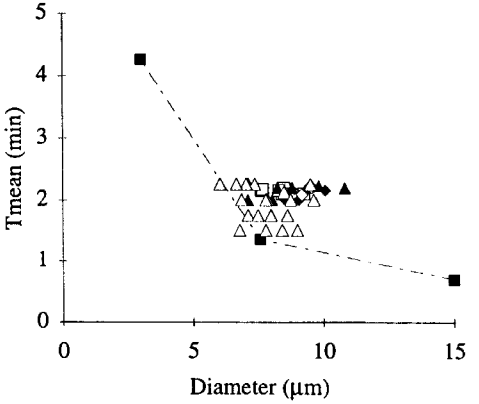

FIG. 11 Fractogram mean time (only data with small variation coefficients have been used) versus particle diameter: (■) latex beads; (▲) L7; (△) L7 (fraction); (□) L10; (◆) L11; (◇) L12.

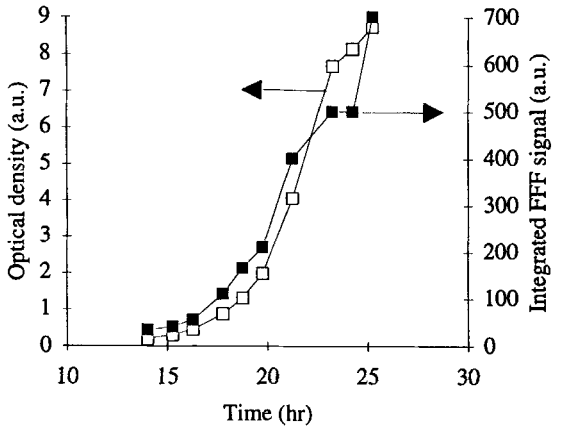

FIG. 12 Broth optical density (□) and integrated FFF signal (■) versus fermentation time for Experiment L7.

concentration at the condition that the integration is performed only on the fractogram part related to entire cells. It should be noticed, however, that FFF requires a high dilution of the broth, higher than for optical density, which may introduce a large error in the biomass concentration.

CONCLUSION

Asymmetrical flow FFF was applied to samples of full fermentation broth of *Saccharomyces cerevisiae* during their growth on glucose. In the early stages of fermentation, the lift-hyperlayer mode applies to intact cells. The operation conditions used here did not permit a complete separation between single cells and doublets: the resolution of the method should be improved to reach such a goal. When the culture gets older, macromolecules are dispersed into the broth due to cell lysis and they are eluted according to the normal mode.

Fractograms T_{mean} and T_{mode} can be used to assess the culture status; any large discrepancy between them is an indication of the culture decay. Furthermore, integration of the part of the signal relative to full cells should give a better estimation of the cell mass as compared to optical density of the full broth as cell fragments are not taken into account.

It was also demonstrated that image analysis data provide a possibility to calibrate the FFF system when no suitable standards are available.

Although the method needs refinements to improve cell samples fractionation, asymmetrical flow FFF is a fast technique of reasonable cost

(similar to HPLC) which could be used to monitor cell lysis and separate different types of cells under near native conditions, which could permit their reculture later on.

REFERENCES

1. J. C. Giddings, "Field Flow Fractionation: Analysis of Macromolecules, Colloidal and Particulate materials," *Science*, *260*(5113), 1456–1465 (1993).
2. J. C. Giddings, F. J. Yang, and M. N. Myers, "Flow Field-Flow Fractionation as a Methodology for Protein Separation and Characterization," *Anal. Biochem.*, *81*, 395–407 (1977).
3. J. C. Giddings, M. A. Benincasa, M. K. Liu, and P. Li, "Separation of Water-Soluble Synthetic and Biological Macromolecules by Flow FFF," *J. Liq. Chromatogr.*, *15*(10), 1729–1747 (1992).
4. J. C. Giddings, F. J. Yang, and M. N. Myers, "Flow Field-Flow Fractionation: New Method for Separating, Purifying and Characterizing the Diffusivity of Viruses," *J. Virol.*, *21*, 131–138 (1977).
5. A. Litzén, J. K. Walter, H. Krischollek, and K. G. Wahlung, "Separation and Quantitation of Monoclonal Antibody Aggregates by Asymmetrical Flow Field-Flow Fractionation and Comparison to Gel Permeation Chromatography," *Anal. Biochem*, *212*, 469–480 (1993).
6. B. N. Barman, E. R. Ashwood, and J. C. Giddings, "Separation and Size Distribution of Red Blood Cells of diverse Size, Shape and Origin by Flow Hyperlayer Field Flow Fractionation," *Ibid.*, *212*, 35–42 (1993).
7. K. G. Wahlund and A. Litzén, "Application of an Asymmetrical Flow Field-Flow Fractionation Channel to the Separation and Characterization of Proteins, Plasmids, Plasmid Fragments, Polysaccharides and Unicellular Algae," *J. Chromatogr.*, *461*, 73–87 (1989).
8. M. N. Pons., H. Vivier, J. F. Rémy, and J. A. Dodds, "Morphology Characterization of Yeast by Image Analysis during Alcoholic Fermentation," *Biotechnol. Bioeng.*, *42*, 1352–1359 (1993).

Received by editor August 12, 1996
Revision received November 1996